Catalytic Reduction Performance of Carboxylated Alginic Acid Derivatives

Raed H. Althomali
King Abdulaziz University
Khalid A. Alamry
King Abdulaziz University
Mahmoud Hussein Abdo (mahussein74@yahoo.com)
King Abdulaziz University https://orcid.org/0000-0002-5128-5136
Shams H. Abdel-Hafez
King Abdulaziz University

Research Article

Keywords: Spectrophotometer analysis, Metal coordinate, Carboxylated alginic acid, Catalytic Reduction

Posted Date: November 29th, 2021

DOI: https://doi.org/10.21203/rs.3.rs-1098571/v1

Abstract

In this study, the catalytic reduction behavior of carboxylated alginic acid derivatives has been investigated against the harmful organic dyes including Methyl Orange (MO) and Congo Red (CR). Alginic acid was firstly oxidized through an easy addition of $KMnO_4$ as an oxidizing agent. A carboxylated alginic acid (CAA) has been interacted with selected metal ions (Sn, Fe, Ni, and Zr) through coordination bonds at the value of pH = 4 to form the corresponding metal complexes namely: Sn-CAA, Fe-CAA, Ni-CAA and Zr-CAA. The consistency of the coordination was confirmed by several spectroscopic techniques including FT-IR, XRD, SEM, and EDX. The catalytic reduction of these metal ion-based products was carried out against MO and CR in the presence of $NaBH_4$ as a reducing agent under UV irradiation. All catalysts based metal complexes showed enhanced catalytic reduction against CR compared to MO. Among all those mentioned metal complexes Sn-CAA showed the best catalytic reduction of these dyes. The time taken by the Sn-CAA for CR, and MO is 5 and 7min respectively. Ni-CAA was classified as the second efficient product against both dyes, where the reduction process took 20 and 9 min respectively. The other two catalysts took a long time for CR and MO reduction. Zr-CAA showed more than 80 % reduction of only CR dye within 20 min. Whereas, Fe-CAA did not show any significant sign of reduction against both the dyes after the same time. The order of higher catalytic reduction was illustrated as: Sn-CAA > Ni-CAA > Zr-CAA = Fe-CAA.

1. Introduction

Nowadays, the use of biopolymer as a catalyst is increased due to minimizing the procedure expense and make several applications more practicable and environmentally friendly. The biopolymers such as chitosan (CS) [1],starch [2], alginate and cellulose [3] etc. have been extensively utilized as heterogeneous green catalysts in the chemical transformations. Furthermore, supramolecular designs of usual carbohydrates in recent times attracted much attention as “smart materials” from bio and nano engineering perspectives. These polymers contain various functionalities that exhibit good catalytic applications. When looking at the structure of alginic acid it comprises of homopolymeric blocks of 1-4-linked β-D-mannuronic acid (M) and R-L-guluronic acid (G). Both the acidic units M and G were joined with areas of alternating structure in variable proportions of MG, GG and MM blocks.[4] Moreover, the eye-catching structures of AA are reactive carboxyl and hydroxyl functional groups. This feature made the composition as a template for synthesizing metal coordinate. The functionalization of the polymer material will rise its choosiness towards a specific ion. Permissible to efficiently exploit the hydroxyl groups in the alginic acid an oxidation reaction was performed by means of potassium permanganate ($KMnO_4$), which alters the hydroxyl groups of AA into carboxyl groups namely carboxylated Alginic Acid (CAA)[5–9]. The choice of a biopolymer for instance AA has specific applications like photo-luminesce, biocompatibility and conductivity, which is really essential, and could be utilized in place of different technological purposes. As a result of the existence of carboxylic and hydroxyl group in its main sequence it shows exceptional films forming, membrane, fibers, and gels abilities [10]. The higher valence

metal ions amalgamated materials remain fixated to prepare novel composite having respectable performances like removal and catalytic applications etc.[5]

There are many types of synthetic dyes used yearly in millions of tons by the industries [11]. During the dyeing process, many color pigments released into the water reservoir from paper, garments, and pharmaceuticals industries etc. to make water polluted and toxic for the surrounding environment. The strong color of azo dyes is because in their chemical formula they contain (–N=N–) groups[12–13]. The azo compounds contain the biggest group of synthetic organic dyes and hugely utilized in food, paper, textile and cosmetic industries. Among them, MO has been widely utilized in laboratories as an indicator and in plastics, paper, textile, cosmetics, rubber, pharmaceuticals and printing industries [14–15]. The azo group present in MO lowers its biodegradability and makes it harmful to the ecosystem. It causes severe health problems like diarrhea, vomiting, and nausea [16]. For that reason, eliminating and reduction MO dye from water ecosystem is necessary. Previously, there were a lot of interest arises in hydrogenation of catalyst and heterogeneous catalysis [17–18]. Amongst the disclosed industries, fabric industry arises as a first rank for coloration of fibers, clothes etc. in using dye molecules. Even though, it's really tough to eliminate industrialized azo-dyes wastes from water and the utmost techniques utilized for treating the industrial effluents are catalysis, ion exchange, chemical coagulation, flocculation, precipitation, adsorption, biological degradation, membrane filtration, and adsorption using active carbon treatment, ozonation, denitrification process[19] electro-Fenton degradation [20] electrochemical sensor etc. Moreover, among them catalysis shows very good activity for reducing these dyes., As a continuation of our research for the fabrication of different types of hybrid nanocomposite materials for the eco-friendly applications, we giveaway easy and a simple process, i.e. aqueous phase preparation of M-CAA by means of natural stuffs such as seaweeds obtained as a low cost, eco-friendly in addition to reducing agents. The prime theme of our present work was to accomplish a catalytic effectiveness of natural products as a catalyst in the reduction of commercially available carcinogenic Congo Red (CR) and methyl orange (MO) as azo dyes from the aqueous solution functionalized and metal coordinated biomaterials as catalysts to reduce these harmful organic dyes.

1. Experimental

2.1. Chemicals and reagents

Potassium permanganate ($KMnO_4$), hydrochloric acid (HCl), sulfuric acid (H_2SO_4). Sodium hydroxide (NaOH), potassium dichromate ($K_2Cr_2O_7$), $SnCl_2{\cdot}2H_2O$, $NiCl_2.4H_2O$, $FeCl_2.2H_2O$, $ZrOCl_2.8H_2O$. Sodium borohydride ($NaBH_4$, 99%) Alginic acid (AA), were obtained from BDH chemicals Ltd Poole England. From Merck (Germany) MO and CR azo dyes were bought. Solvents and chemicals utilized were of analytical grades without further treatment. Deionized water obtained from Milli-Q Plus system (Millipore, Bedford, MA, USA).

2.2 Characterization

All spectrophotometric measurements recorded with UV-visible spectrophotometer (Shimadzu 1800) with a 10 mm (path width) quartz cell. Orion pH meter (model EA 940) was employed for the test solutions and pH measurements and a digital micropipette (Volac) for the preparation all solution. Deionized water obtained from Milli-Q Plus system (Millipore, Bedford, MA, USA) and used for the preparation of solutions. field emission scanning electron microscope (FESEM) (JSM-7600 F, USA) for morphological studies also for elemental studies were carried out with energy dispersive x-ray spectroscope (EDX) fitted to FESEM and x-ray photoelectron spectroscope. Fourier transform infrared (FTIR) spectroscope (Thermo scientific, USA) for collection of FTIR spectra data (Range: 500-4000 cm^{-1}).

2.3 Preparation of coordinated M –CAA

For oxidizing alginic acid (5g), it was treated with an oxidizing agent potassium permanganate having concentration of 10mM. The process was done under strong mechanical strring for 30 min at temperature range of 45°C. Due to the explosive nature of potassium permanganate, it was used within the range of 10mM as reported earlier [12]. The polymer solution goes under centrifugation to obtained CAA. The material was thoroughly washed with distilled water to reach the pH up to 6-7. The CAA dried in oven for 2h at 60°C. To prepared the metal coordinates of CAA with Ni^{+2}, Zr^{+4}, Sn^{+2}, and Fe^{+2} metals, two round bottom flasks were taken and each one contain 2g CAA in 100ml DI water. It was than treated with 0.2 mol of metal solution ($NiCl_2.4H_2O$, $ZrOCl_2{\cdot}8H_2O$, $SnCl_2{\cdot}2H_2O$ and $FeCl_2.H_2O$). The mixture was stir continuously for 24h at RT. For metal complexation, to keep the pH around four. The solution mixtures were treated with aqueous solutions of (1M) H_2SO_4 and NaOH. The final product obtained after filtration washed vigorously by DI water and keep in oven for 4 h for drying at 60° C.

3. Results And Discussions

3.1 FT-IR Fourier-transform infrared spectroscopy

After doing oxidation of the AA, we checked the formation of carboxyl group by FTIR. The peak at around 1745cm^{-1} shown in Fig. (1b) is coming from carbonyl group present in AA after oxidation. At around 3000-3500cm^{-1} we can clearly observed the fall in intensity of peak in fig. (1b) from the parent material i.e. AA Fig. (1a) which confirms the formation of the carbonyl group to AA. During the meantime we also treat the CAA with metals as well and to check the formation of the coordinate bond with metals. When the coordinate bond formed between metal and CAA the intensity at around 1745cm^{-1} disappeared Fig. (c-f), and again it shows broad peak at around 3000-3500cm^{-1}.This approves that protons that are in the carboxylic acid had changed and formed a harmonic bond with metals[31-32].

3.2 The X-ray diffraction (XRD) of CAA and M-CAA

To carry out X-ray diffraction pattern for studying the lattice structure of CAA and M-CAA adsorption materials. Fig. 2 shows the XRD spectra of CAA (a), Zr-CAA (b), Sn-CAA(c) and (d) Ni-CAA respectively. The distinguished crystalline peaks of CAA(a) were located at 14.47° and 21.31°, respectively,

representing the reflections of the (422) and (511) planes Fig (2a) [33]. The XRD pattern analysis of Zr-CAA Fig (2b) showed that there was a tetragonal phase of Sn and Ni Fig (a-d). The analysis also confirmed the semi-crystalline nature, which improved the structural stability of the manufactured M-CAA adsorbent material.

3.3. Scanning electron microscopy (SEM) image and EDAX for CAA, Sn^{+2} and $Zr^{+4}Ni^{+2}$, Fe^{+2}

By checking the FE-SEM pictures shown in Fig 3, the morphology of net CAA and Zr-CAA as a selected example can be clarified. The SEM images a, b represents the CAA surface which consists of aggregated tiny particles in both lower and medium magnifications which is in accordance with the literature[34]. The images from (c, d) represent from medium to high magnifications of Zr-CAA (x =7,500 and 60,000) respectively. The medium magnification shows the surface consists of sponge like shape; while the resultant high magnification image (x = 60,000) shows accumulative tiny spherical particles in the nanoscale. The complex mechanism between the selected metal cation and CAA can be used to explain the difference in morphological structure formed in these imaged compare to the reported images for pure CAA [34]. These tiny points indicate Zr are effective in coordination with CAA. The Zr-CAA images give a good evidence for the complexation process throughout metal ion chelation. However, the reported CAA images undoubtedly demonstrates a complete different morphological features than that observed in this text. Furthermore, the synthesized Zr-CAA selected sample has been further investigated by EDS analyses to quantitatively defined the elemental composition. The Zr were undoubtedly spotted in Zr-CAA formulation. Zr alongside C and O detected in Zr-CAA, proposing the effective formation of Zr-CAA. C and O elements were detected due to the presence of carboxylic alginic acid. Zr was identified along with C, and O in Zr-CAA catalyst and the weight percentage for C, O and Zr in the form of Zr-CAA is 54, 44 and 2% respectively.

3.4. Catalytic study

Due to the diverse application of dyes and their unhealthy effect on the surrounding environment and aquatic life, we select two anionic dyes MO and CR for our study. We prepared a facile method for the reduction of these dyes. The CAA metal coordinate complex utilized as a catalyst in the presence of a reducing agent using UV-vis spectrometer technique in the wavelength range of 200-800 nm. To know the catalytic activity of the catalyst against model reaction of CR and MO we prepared fresh sodium borohydride having concentration of 0.1M. We took 2.5ml of dyes in cuvette, take the reading after that we add 0.5ml of reducing agent sodium borohydride, and measured it. Then 10mg of metal catalyst immersed in a cuvette and MO at 468 nm and CR at 495 nm. The time interval for the reaction was 1min. The calculation of reduction of these dyes done according to time and percentage reduction equation as follows,

$$\%Red = \frac{A0-A}{A0} \times 100 = \frac{C0-C}{C0} \times 100 \qquad (1)$$

Where A_0 is the UV-vis absorption intensity of dyes at time t=0, and A is the UV–vis absorption of same solution at time t (min). C_0 is initial concentration of the dyes and C is the concentration after time' t'. Dyes reduction was carried out according to the proposed mechanism, as Figure 4

3.4.1 Evaluation of M-CAA toward CR and MO

The selection of materials and their nature and chemical properties are important for many different applications, especially water purification. Therefore, it is necessary to choose materials with unique properties in terms of efficiency in their work as well as their cost and have an anti-bacterial feature. Many applications and researches applied to water purification. Nevertheless, all methods have a cost and may require high-cost devices, which makes their efficiency in the end less than Less than hoped for in the process of purifying the water from toxic material such as azo dyes. The method of catalytic reduction of dyes is a simple and easy method. In addition, many nanoscale materials used to remove dyes or even reduce them, but there are some disadvantages to them, which is the difficulty of removing them from the water, which requires difficult techniques or even filtering it to get rid of them. All these are defects of some of the materials mentioned. polysccride such as chitosan or carboxymethylcellulose. They have been used to reduction dyes in many literatures because of the properties that make it easy to get rid of them after use.in this study, in this work The carboxylated alginic acid CAA used as a safe organic biopolymer that contains many active groups that are important in interaction with metals as coordinate bonding for reduction harmful anionic azo dyes. Through the experiment in Fig 4a and 7a we found that AA and ($NaBH_4$) without modification does not more effect on ionic dyes because they both carry the same electrical charge also, when CAA and ($NaBH_4$). There were more effective groups such as the carbonyl group and hydroxyl, but in the process of studying it with harmful dyes such as M.O and C.R, the result was unsatisfactory due to the presence of high electrical charges on many hydroxyl and carbonyl groups as Fig 4b and 7b. Similar to the charge carried by the dyes thus there was no significant effect on the reduction reaction.

3.4.1.1. Catalytic reduction of CR

An anionic diazo dye, which is widely utilized in various industries, is Congo red (CR). Because of its utilization in various fields like textile, cotton, silk, food, paper and pulp manufacturing factories, CR is very important in various azo dyes. It's utilization in medical field as a biological stain for the identification of amyloidosis, and as an pointer in acidic media [35-36]. In addition to the extensive uses of CR, it also has toxic effects on wildlife. CR can cause vomiting, gastrointestinal irritation, skin and eye irritation, diarrhea, etc. In women it causes liver tumors for exposing long-term to CR [37-38]. CR could report allergic reaction. The CR disposal rate is extraordinary in the use and manufacturing procedure. Traditional treatments cannot effectively remove CR. In addition, under anaerobic conditions, CR digested into human carcinogen called benzidine [38-39] .

The reduction of CR takes place in the existence of M-CAA and $NaBH_4$. For reducing, 2.5 ml of 0.13 mM CR solution was placed in a quartz cuvette and add 0.5 ml of $NaBH_4$ into the solution. CR shows two

strong absorption peaks in the UV-visible spectrum at 493 and 344 nm. In the absence of a catalyst, the peak intensity does not change for AA as shown in Fig 5a. We than modify the AA to CAA and again check the UV for CR it also shows similar result like its predecessor Fig. 5b. After that, we make coordinate complex of CAA with metals like Sn, Fe, Zr and Ni (M-CAA).

By adding 10 mg of M-CAA, the peak intensities at 493 and 344 nm begin to decline. As shown in Fig 6a-d, the decrease in CR was recorded by measuring its UV-vis spectrum at regular time interval of 1 min between the two measurements. Adding of M-CAA reduces both peak intensities. Though, as the intensity increases, a fresh peak arises at 252 nm, as displayed in Fig (6a, c, d). Therefore, the steady vanishing of peaks at 493 and 344 nm is because of CR reduction. Therefore, the arise of a new peak at 252 nm is due to the formation of free amino group compounds in the course of the reduction process of CR. The reduction CR was done against different metal catalyst like Fig 6 Sn-CAA (a), Fe-CAA(b), Ni-CAA(c)and Zr-CAA(d)respectively. Among them Sn-CAA shows the best result as it reduction the CR in 5 min while the others show long time for reduction. Fe-CAA took 20 min but did not show any effect of reduction, Ni-CAA took 9 min to reduce more than 95% and Zr-CAA took 27 min to reduce the CR up to 85%.

The percentage reduction of CR was measured as of the map of the UV-vis spectrum by means of equation (1). At this point, in the presence of $NaBH_4$ and M-CAA, CR was reduced completely as shown in Fig 7a. According to the earlier reports, $NaBH_4$ alone does not show any effect on CR, even when utilized in excess[40]. Thus, the overall reduction process of the CR monitors the pseudo-first order kinetics. The calculation of the rate constant (K_{app}) was based on the relationship between $\ln(A_t/A_0)$ and the reduction time (as shown in Fig (7b) by formula (1). The calculation done for K_{app} from the slope of CR existed as K_{app}= 0.6602 for Sn and K_{app}= 0.427 of Ni and K_{app}= 0.173. Zr and K_{app}= 0.173 for Fe.

3.4.1.2. Catalytic reduction of MO

With the growth of industry, human beings are facing severe environmental problems because of releasing enormous number of pollutants into the water-based environment, particularly dyes and other organic molecules. The ejection of sewage into the ecological unit is a chief hazard to marine ecosystem and human health. The presence of azo (–N=N–) group in chemical structure of the dyes gives them deep color [12-13]. Amongst organic synthetic dyes, azo group has established a major class of dyes and is extensively exploited by means of textile, food, cosmetic, paper and pulp manufacturing factories. MO is also anionic azo dye often utilized as an indicting material in laboratories and in the paper, textile, cosmetics, rubber and pharmaceutical industries etc [14-15].

Emission of azo dye unwanted liquid from numerous industries, exclusively the textile industry, into the aquatic ecosystem pose a thoughtful warning. Therefore, the improvement of fresh methods intended for the decomposition of diazo has attracted boundless attention. The MO has intense peak around 468 nm. According to earlier reports, $NaBH_4$ alone can reduce MO dye thermodynamically which is beneficial but the reaction is very gentle kinetically [41]. Lack of an appropriate catalyst, even within a few hours, the peak intensity at 468 nm peak of MO remained constant [42-43].

MO was strong absorption peak in the UV-visible spectrum at 468 nm. In the absence of a catalyst, the peak intensity does not change for AA as shown in Fig 8a. We than modify the AA to CAA and again check the UV for MO it also shows similar result like its predecessor Fig. 8b. In order to catalytically reduce MO, first put 2.5ml of dye solution into the quartz cuvette and then add 0.5ml of $NaBH_4$ having 0.1M concentration. The UV-vis spectrum of MO shows an intense peak at around 468 nm. Before adding the catalyst, the peak intensity of MO remains intact at 468nm. Though, after introducing 10mg of metal catalyst, the peak intensity at around 468nm began to decrease.

As shown in Fig 9(a-d), the catalytic study of M-CAA was measured by assessing the UV-vis spectrum using a time span of 1 min. By adding M-CAA, the decrease in intensity of peak at 468 nm was observed. Therefore, the steady vanishing of the peak around 468 nm because of reducing the MO, usually in the existence of a vigorous catalytic agent, $NaBH_4$ reduces MO molecules at the azo spot by producing low molecular free amino group compounds. Therefore, during MO reduction process, the formation of free amino compounds is the reason for the creation of a new peak at 250 nm.

The effectiveness of (M-CAA) has been tested with the aforementioned metals. Below we see the figures for each metals and the extent of its effect on the dyes M.O, and we conclude from them that the Sn is the best metal, as we see that it did not take much time less than 7 min in the process of reducing MO dye compared to the rest of the metals (Ni, Fe, Zr) which take more time in Ni cause 20 min but for Fe and Zr not more effect as Fig 9a, d.

The apparent rate constant (K_{app}) calculation was based on the relationship between $\ln(A_t/A_0)$ and the reduction time as shown in Fig 10 by formula (1). The calculation done for K_{app} from the slope of MO was K_{app}= 1.44 for Sn and K_{app}= 0.0413 of Ni and K_{app}= 0.14. Zr and K_{app}= 0.139 for Fe.

3.4.2. Catalytic reduction of mixed solution of M.O and CR with Sn-CAA

Through the previous results, we obtained detailed information about the two dyes through Sn-CAA. We mixed the two dyes with 10ml of 0.1mM of each CR and MO solution, and then added 2.5ml of the mixed in the UV cuvette, (0.1 M) 0.5 ml $NaBH_4$ and 10mg of Sn-CAA for analysis. Under the same conditions of testing the two dyes separately, a decrease in the absorption of the UV spectrum is observed every minute. So, when the two dyes are mixed, we have one peak, and it is broad and large, which indicates that the two peaks overlap because they are both close to aggregate absorption (465 nm and 495 nm MO and CR, respectively**.** When the two dyes are added with Sn-CAA, they will affect the reduction process in a short time of less than about 6 minutes. We can see that the peak intensity decreases at 476 and 344 nm, and with increasing, at 252 nm A new peak appears with very high intensity, because free amino compounds are formed during the reduction of CR and MO, which shows the effectiveness of Sn-CAA in the reduction process, and even the two dyes together show excellent performance, as shown in Fig 11. The apparent rate constant (K_{app}) calculation was based on the relationship between $\ln(A_t/A_0)$ and the reduction time (as shown in Fig 11(c) by formula (1). The K_{app} measured from the slope of CR was K_{app}= 0.598.

3.4.3. Recyclability

The recyclability of Sn-CAA as a coordination bond was determined. Following the same experimental procedure as before to reduce C.R and M.O. We used the same carboxylated Sn-CAA, washed with water, and reused in seven reductions of C.R and M.O solutions. In the course of seven uses of coordinated carboxylated alginic acid, a reduction of more than 90% was observed. In Fig 12 you can see the time taken to reduce the CR and MO solutions to more than 90% in the first, second, third, fourth, fifth, sixth, and seventh cycles. For the MO solution, in the 90% reduction process, the reduction was completed in less than 7 minutes. The first cycle takes 7 while 9, 11, 13, 13, and 15 minutes for the other cycles. In the case of C.R, 90% of the reduction reaction can be completed in 5 minutes, while most of the conversion in the repeated cycle is completed in 5, 7, 10, 11, and 11 minutes. We have observed that the reduction time increases when using the same Sn-CAA, which indicates a decrease in catalytic performance. Furthermore, a comparison table regarding the using of different matrices against the reduction of CR and MO at 25 °C has been listed in Table 1.

Table 1: Comparison table of different matrices for reducing CR and MO at 25 °C

Matrix	Target Pollutant	Time reduction	. Reducing agent	K_{app} (min^{-1})	Ref
Cu NPs/MPs	Congo Red	7.0	$NaBH_4$	0.610	44
Au NPs-Dp-p(El) membrane	Congo Red	29	$NaBH_4$	0.209	45
Gold Nanoparticles (AgNPs)	Congo Red	15	$NaBH_4$	-	46
N-doped Carbon Nano dots	Congo Red	10	$NaBH_4$	0.314	47, 48
Sn-CAA	Congo Red	6	$NaBH_4$	0.66	This work
Chitosan coated cellulose paper	Methyl orang	10	$NaBH_4$	0.116	49
DLP-AuNPs	Methyl orang	8	$NaBH_4$	0.017	50, 51
Ag NPs	Methyl orang	21	$NaBH_4$	0.1931	52, 53
Fe3O4@His@Ag	Methyl orang	8	$NaBH_4$	0.423	54, 55
Sn-CAA	Methyl orang	6	$NaBH_4$	1.44	This work

4. Conclusion

Safe, low costly and ecofriendly modified alginic acid derivatives in the form of M-CAA were successfully prepared as coordinate materials including different metal ions (Sn, Fe, Ni and Zr). The desired materials were prepared by easy method using two steps. The final products were confirmed by common characterization techniques including FT-IR, XRD, SEM and EDX analyses. These materials were applied as moderate new materials for the catalytic reduction of both (M.O, C.R) dyes. Sn-CAA showed the best catalytic reduction for CR and MO (5 and 7min) respectively. Whereas, Fe-CAA and Zr-CAA showed the longest catalytic reduction time against the same dyes. The optimum conditions for all the used catalysts were measured. Sn-CAA catalytic reduction showed an efficient recyclable product after 4 cycles then

gradually become less efficient. Furthermore, Sn-CAA showed an excellent result for purifying natural water from toxic organic wastes as an example for real test sample.

Declarations

Acknowledgment

Taif University supporting project number (TURSP-2020/23), Taif University, Taif, Saudi Arabia.

References

1. Al-Matar, H. M.; Khalil, K. D.; Meier, H.; Kolshorn, H.; Elnagdi, M. H., Chitosan as heterogeneous catalyst in Michael additions: The reaction of cinnamonitriles with active methylene moieties and phenols. *Arkivoc* **2008,** *16*, 288-301.

2. Ren, Z.; Zhang, G.; Chen, J. P., Adsorptive removal of arsenic from water by an iron–zirconium binary oxide adsorbent. *Journal of colloid and interface science* **2011,** *358* (1), 230-237.

3. Safari, J.; Banitaba, S. H.; Khalili, S. D., Cellulose sulfuric acid catalyzed multicomponent reaction for efficient synthesis of 1, 4-dihydropyridines via unsymmetrical Hantzsch reaction in aqueous media. *Journal of Molecular Catalysis A: Chemical* **2011,** *335* (1-2), 46-50.

4. Saha, S.; Pal, A.; Kundu, S.; Basu, S.; Pal, T., Photochemical Green Synthesis of Calcium-Alginate-Stabilized Ag and Au Nanoparticles and Their Catalytic Application to 4-Nitrophenol Reduction. *Langmuir* **2010,** *26* (4), 2885-2893.

5. Pandi, K.; Viswanathan, N., A novel metal coordination enabled in carboxylated alginic acid for effective fluoride removal. *Carbohydrate polymers* **2015,** *118*, 242-249.

6. Paudyal, H.; Pangeni, B.; Inoue, K.; Kawakita, H.; Ohto, K.; Ghimire, K. N.; Alam, S., Preparation of novel alginate based anion exchanger from Ulva japonica and its application for the removal of trace concentrations of fluoride from water. *Bioresource Technology* **2013,** *148*, 221-227.

7. Viswanathan, N.; Meenakshi, S., *Enhanced fluoride sorption using La(III) incorporated carboxylated chitosan beads*.

8. Viswanathan, N.; Meenakshi, S., Enhanced and selective fluoride sorption on Ce (III) encapsulated chitosan polymeric matrix. *Journal of applied polymer science* **2009,** *112* (3), 1114-1121.

9. Jeon, C.; Park, J. Y.; Yoo, Y. J., Characteristics of metal removal using carboxylated alginic acid. *Water Research* **2002,** *36* (7), 1814-1824.

10. Unal, B.; Toprak, M. S.; Durmus, Z.; Sözeri, H.; Baykal, A., Synthesis, structural and conductivity characterization of alginic acid–Fe3O4 nanocomposite. *Journal of Nanoparticle Research* **2010,** *12* (8),

3039-3048.

11. Almeida, E.; Corso, C., Decolorization and removal of toxicity of textile azo dyes using fungal biomass pelletized. *International journal of environmental science and technology* **2019,** *16* (3), 1319-1328.

12. Y. El maguana , N. Elhadiri, M. Benchanaa, and R. Chikri. Adsorption Thermodynamic and Kinetic Studies of Methyl Orange onto Sugar Scum Powder as a Low-Cost Inorganic Adsorbent. Journal of Chemistry Volume **2020**, 9165874, 10 pages (1-10).

13. Tajbakhsh, M.; Alinezhad, H.; Nasrollahzadeh, M.; Kamali, T. A., Green synthesis of the Ag/HZSM-5 nanocomposite by using Euphorbia heterophylla leaf extract: a recoverable catalyst for reduction of organic dyes. *Journal of Alloys and Compounds* **2016,** *685*, 258-265.

14. León, G.; García, F.; Miguel, B.; Bayo, J., Equilibrium, kinetic and thermodynamic studies of methyl orange removal by adsorption onto granular activated carbon. *Desalination and Water Treatment* **2016,** *57* (36), 17104-17117.

15. Omidvar, A.; Jaleh, B.; Nasrollahzadeh, M.; Dasmeh, H. R., Fabrication, characterization and application of GO/Fe3O4/Pd nanocomposite as a magnetically separable and reusable catalyst for the reduction of organic dyes. *Chemical Engineering Research and Design* **2017,** *121*, 339-347.

16. Munagapati, V. S.; Yarramuthi, V.; Kim, D.-S., Methyl orange removal from aqueous solution using goethite, chitosan beads and goethite impregnated with chitosan beads. *Journal of Molecular Liquids* **2017,** *240*, 329-339.

17. Maryami, M.; Nasrollahzadeh, M.; Sajadi, S. M., Green synthesis of the Pd/perlite nanocomposite using Euphorbia neriifolia L. leaf extract and evaluation of its catalytic activity. *Separation and Purification Technology* **2017,** *184*, 298-307.

18. Nasrollahzadeh, M.; Issaabadi, Z.; Sajadi, S. M., Green synthesis of Pd/Fe3O4 nanocomposite using Hibiscus tiliaceus L. extract and its application for reductive catalysis of Cr (VI) and nitro compounds. *Separation and Purification Technology* **2018,** *197*, 253-260.

19. Kulkarni, P., Nitrophenol removal by simultaneous nitrification denitrification (SND) using T. pantotropha in sequencing batch reactors (SBR). *Bioresource technology* **2013,** *128*, 273-280.

20. Oturan, M. A.; Peiroten, J.; Chartrin, P.; Acher, A. J., Complete destruction of p-nitrophenol in aqueous medium by electro-Fenton method. *Environmental Science & Technology* **2000,** *34* (16), 3474-3479.

21. M. A. Hussein, Eco-Friendly Polythiophene(keto-amine)sBased on Cyclopentanone Moiety for Environmental Remediation, J. Polym. Environ., **2018**, 26(3), 1194–1205.

22. D.F. Katowah, G.I. Mohammed, D.A. Al-Eryani, T.R. Sobahi, M.A. Hussein, Rapid and sensitive electrochemical sensor of cross-linked polyaniline/oxidized carbon nanomaterials core-shell

nanocomposites for determination of 2,4-dichlorophenol. *PLoS ONE* **2020**, 15(6),e0234815.

23. D.F. Katowah, G.I. Mohammed, D.A. Al-Eryani, O.I. Osman, T.R. Sobahi, M.A. Hussein, Fabrication of conductive cross-linked polyaniline/G-MWCNTS core-shell nanocomposite: A selective sensor for trace determination of chlorophenol in water samples. *Polymers for Advanced Technologies* **2020**, 31(11), 2615-2631.

24. M. A. Hussein, B. M. Abu-Zied, A. M. Asiri, Fabrication of EPYR/GNP/MWCNT carbon-based composite materials for promoted epoxy coating performance. *RSC Advances* **2018**, 8, 23555-23566.

25. A. M. Alosaimi, M. A. Hussein, M. Y. Abdelaal, T. R. Sobahi & H. D. Rozman. Polysulfone/wood flour/organoclay hybrid nanocomposites as efficient eco-friendly materials*. Composite Interfaces,* **2020**, 27(8), 717-736

26. D. F. Katowah, M. A. Hussein, M. M. Rahman, Q. A. Alsulami, M. M. Alam, A. M. Asiri, Fabrication of hybrid PVA-PVC/SnZnOx/SWCNTs nanocomposites as Sn^{2+} ionic probe for environmental safety. *Polym.-plast. Technol. Mater.***2019**, *00*, 1–16.

27. Y. O. Al-Ghamdi, K. A. Alamry, M. A. Hussein, H. M. Marwani, A. M. Asiri. Sulfone-modified chitosan as selective adsorbent for the extraction of toxic Hg(II) metal ions. *Adsorption Science & Technology,* **2019**, *37(1-2),* 139 -159.

28. M. A. Hussein, H. Marwany, K. Alamry, A. M. Asiri, S. A. El-Daly. Surface Selectivity Competition of Newly Synthesized Polyarylidene(keto-amine)s Polymers Toward Different Metal Ions. *J. of Applied Polymer Science,* **2014**, 131(19), 40873 (1-10).

29. R.H. Althomali, K.A. Alamry, M.A. Hussein, A. Khan, S.S. Al-Juaid, A. M. Asiri. Modification of alginic acid for the removal of dyes from aqueous solutions by solid-phase extraction. *International Journal of Environmental Analytical Chemistry*, Article in press (**2020**).

30. Hussein, M. A., Ganash, A. A.; Alqarni, S. A.; Electrochemical sensor-based gold nanoparticle/poly(aniline-co-o-toluidine)/graphene oxide nanocomposite modified electrode for hexavalent chromium detection: a real test sample. *Polymer-Plastics Technology and Materials,* **2019**, 58(13) 1423-1436.

31. Tackett, J. E., FT-IR characterization of metal acetates in aqueous solution. *Applied Spectroscopy* **1989,** *43* (3), 483-489.

32. Papageorgiou, S. K.; Kouvelos, E. P.; Favvas, E. P.; Sapalidis, A. A.; Romanos, G. E.; Katsaros, F. K., Metal–carboxylate interactions in metal–alginate complexes studied with FTIR spectroscopy. *Carbohydrate research* **2010,** *345* (4), 469-473.

33. Zhao, X. H.; Li, Q.; Ma, X. M.; Xiong, Z.; Quan, F. Y.; Xia, Y. Z., Alginate fibers embedded with silver nanoparticles as efficient catalysts for reduction of 4-nitrophenol. *RSC Advances* **2015,** *5* (61), 49534-49540.

34.

35. Ilayaraja, M.; Krishnan, N.; Kannan, R. S., Adsorption of rhodamine-B and Congo red dye from aqueous solution using activated carbon: kinetics, isotherms, and thermodynamics. *IOSR J Environ Sci Toxicol Food Technol* **2013,** *5* (5), 79-89.

36. Dawood, S.; Sen, T. K., Removal of anionic dye Congo red from aqueous solution by raw pine and acid-treated pine cone powder as adsorbent: equilibrium, thermodynamic, kinetics, mechanism and process design. *Water research* **2012,** *46* (6), 1933-1946.

37. Chatterjee, S.; Chatterjee, S.; Chatterjee, B. P.; Guha, A. K., Adsorptive removal of congo red, a carcinogenic textile dye by chitosan hydrobeads: Binding mechanism, equilibrium and kinetics. *Colloids and Surfaces A: Physicochemical and Engineering Aspects* **2007,** *299* (1-3), 146-152.

38. Chen, H.; Zhao, J., Adsorption study for removal of Congo red anionic dye using organo-attapulgite. *Adsorption* **2009,** *15* (4), 381-389.

39. Chatterjee, S.; Lee, D. S.; Lee, M. W.; Woo, S. H., Enhanced adsorption of congo red from aqueous solutions by chitosan hydrogel beads impregnated with cetyl trimethyl ammonium bromide. *Bioresource Technology* **2009,** *100* (11), 2803-2809.

40. Khan, M. S. J.; Kamal, T.; Ali, F.; Asiri, A. M.; Khan, S. B., Chitosan-coated polyurethane sponge supported metal nanoparticles for catalytic reduction of organic pollutants. *International journal of biological macromolecules* **2019,** *132*, 772-783.

41. ur Rehman, S.; Siddiq, M.; Al-Lohedan, H.; Sahiner, N., Cationic microgels embedding metal nanoparticles in the reduction of dyes and nitro-phenols. *Chemical Engineering Journal* **2015,** *265*, 201-209.

42. Kamal, T.; Khan, S. B.; Asiri, A. M., Synthesis of zero-valent Cu nanoparticles in the chitosan coating layer on cellulose microfibers: evaluation of azo dyes catalytic reduction. *Cellulose* **2016,** *23* (3), 1911-1923.

43. Khan, M. M.; Lee, J.; Cho, M. H., Au@ TiO2 nanocomposites for the catalytic degradation of methyl orange and methylene blue: an electron relay effect. *Journal of Industrial and Engineering Chemistry* **2014,** *20* (4), 1584-1590.

44. Ghosh, B. K.; Hazra, S.; Naik, B.; Ghosh, N. N., Preparation of Cu nanoparticle loaded SBA-15 and their excellent catalytic activity in reduction of variety of dyes. *Powder Technology* **2015,** *269*, 371-378.

45. Subair, R.; Tripathi, B. P.; Formanek, P.; Simon, F.; Uhlmann, P.; Stamm, M., Polydopamine modified membranes with in situ synthesized gold nanoparticles for catalytic and environmental applications. *Chemical Engineering Journal* **2016,** *295*, 358-369.

46. Kolya, H.; Maiti, P.; Pandey, A.; Tripathy, T., Green synthesis of silver nanoparticles with antimicrobial and azo dye (Congo red) degradation properties using Amaranthus gangeticus Linn leaf extract. *Journal of Analytical Science and Technology* **2015,** *6* (1), 33.

47. Arul, V.; Chandrasekaran, P.; Sethuraman, M. G., Reduction of Congo red using nitrogen doped fluorescent carbon nanodots obtained from sprout extract of Borassus flabellifer. *Chemical Physics Letters* **2020,** *754*, 137646.

48. Arul, V.; Chandrasekaran, P.; Sethuraman, M., Reduction of Congo Red using Nitrogen Doped Fluorescent Carbon Nanodots obtained from Sprout Extract of Borassus Flabellifer. *Chemical Physics Letters* **2020**, 137646.

49. Kamal, T.; Khan, S. B.; Asiri, A. M., Nickel nanoparticles-chitosan composite coated cellulose filter paper: an efficient and easily recoverable dip-catalyst for pollutants degradation. *Environmental Pollution* **2016,** *218*, 625-633.

50. Umamaheswari, C.; Lakshmanan, A.; Nagarajan, N. S., Green synthesis, characterization and catalytic degradation studies of gold nanoparticles against congo red and methyl orange. *Journal of Photochemistry and Photobiology B: Biology* **2018,** *178*, 33-39.

51. Umamaheswari, C.; Lakshmanan, A.; Nagarajan, N., Green synthesis, characterization and catalytic degradation studies of gold nanoparticles against congo red and methyl orange. *Journal of Photochemistry and Photobiology B: Biology* **2018,** *178*, 33-39.

52. Vidhu, V. K.; Philip, D., Catalytic degradation of organic dyes using biosynthesized silver nanoparticles. *Micron* **2014,** *56*, 54-62.

53. Vidhu, V.; Philip, D., Catalytic degradation of organic dyes using biosynthesized silver nanoparticles. *Micron* **2014,** *56*, 54-62.

54. Amir, M.; Kurtan, U.; Baykal, A., Rapid color degradation of organic dyes by Fe3O4@His@Ag recyclable magnetic nanocatalyst. *Journal of Industrial and Engineering Chemistry* **2015,** *27*, 347-353.

55. Amir, M.; Kurtan, U.; Baykal, A., Rapid color degradation of organic dyes by Fe3O4@ His@ Ag recyclable magnetic nanocatalyst. *Journal of industrial and engineering Chemistry* **2015,** *27*, 347-353.

Figures

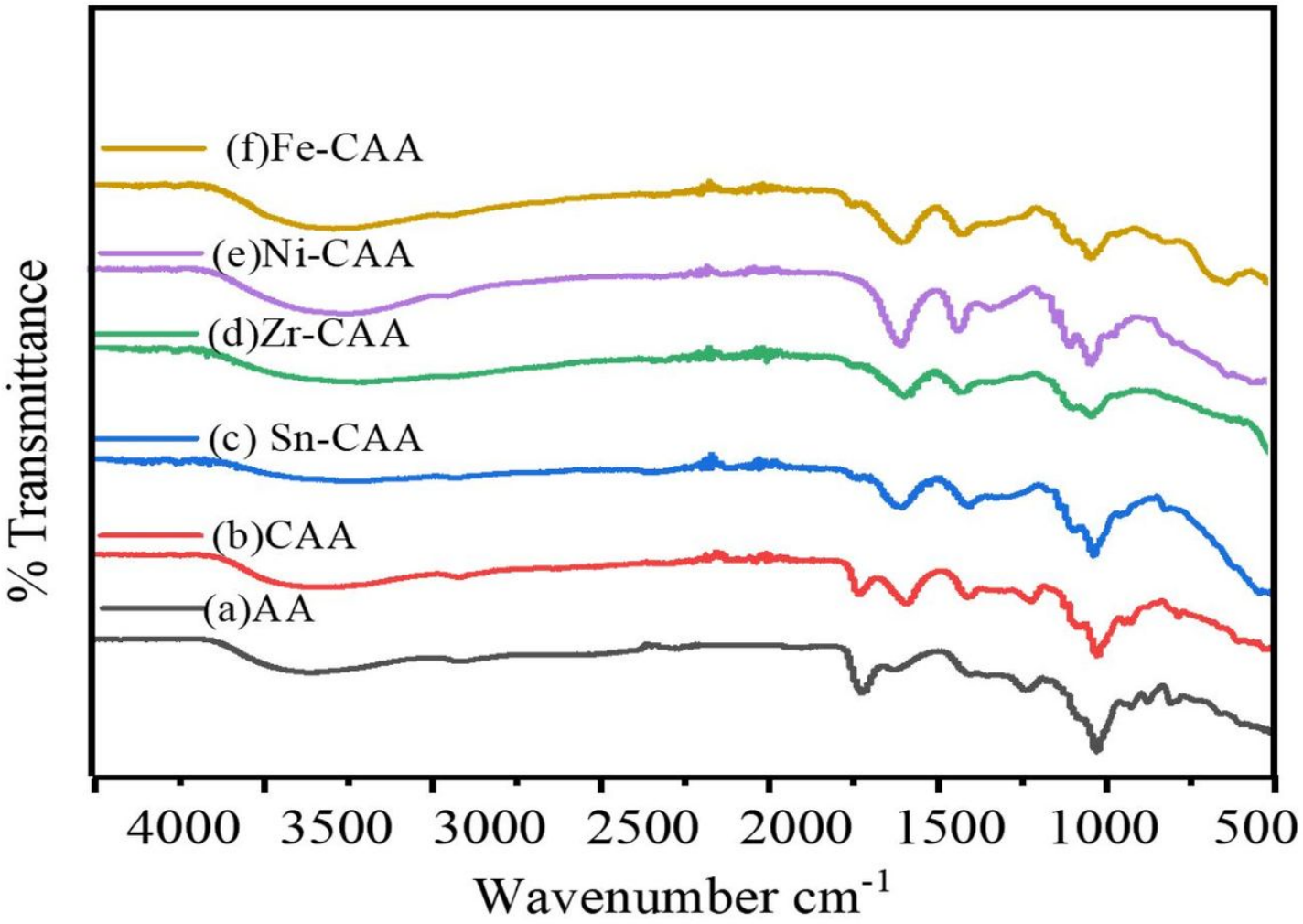

Figure 1

FTIR: (a) AA (b) CAA (c) Sn-CAA (d) Zr-CCA (e) Ni-CAA (f) Fe-CAA

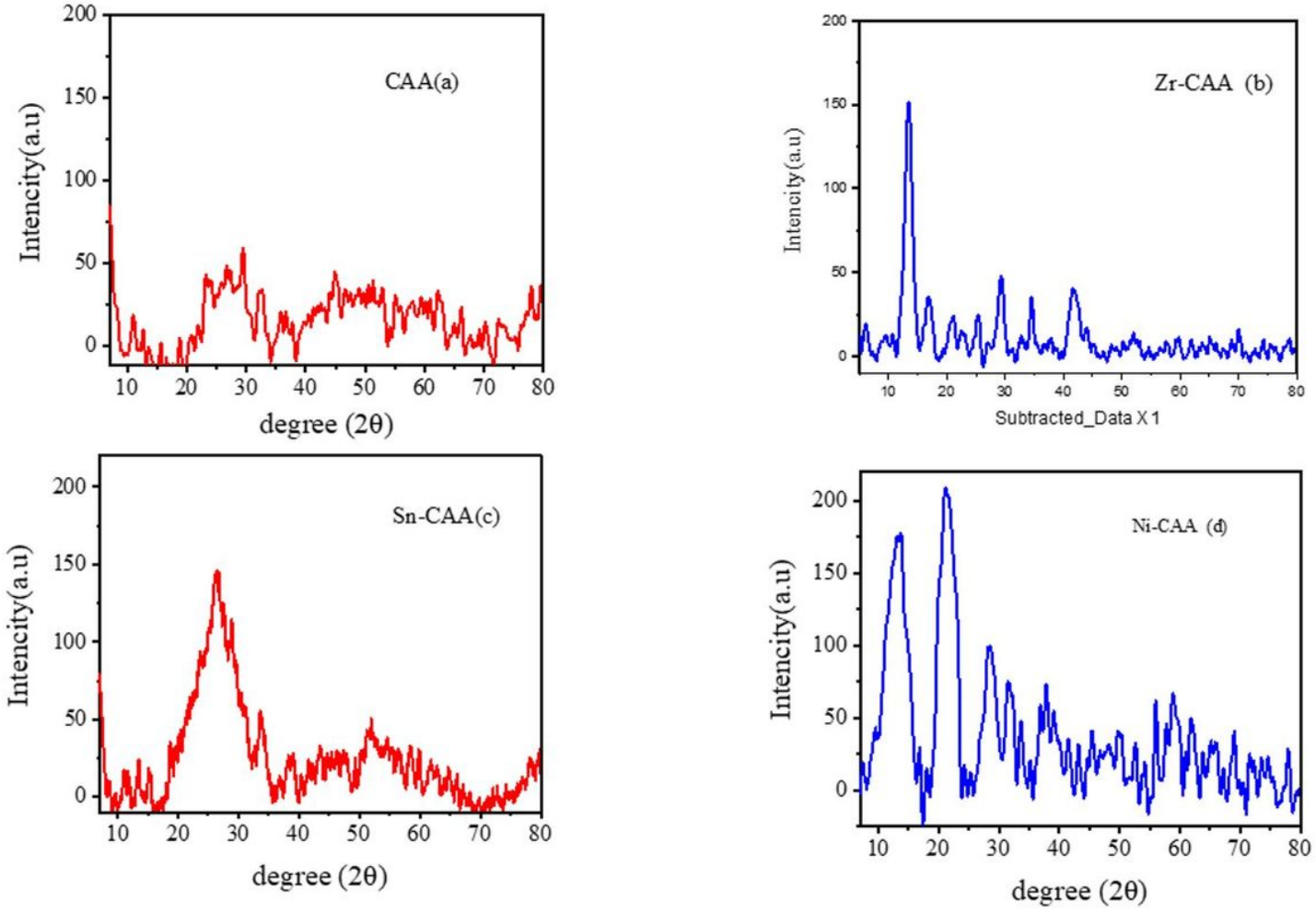

Figure 2

XRD patterns of (a) CAA and (b) Zr -CAA (c) Sn-CAA (d) Ni-CAA

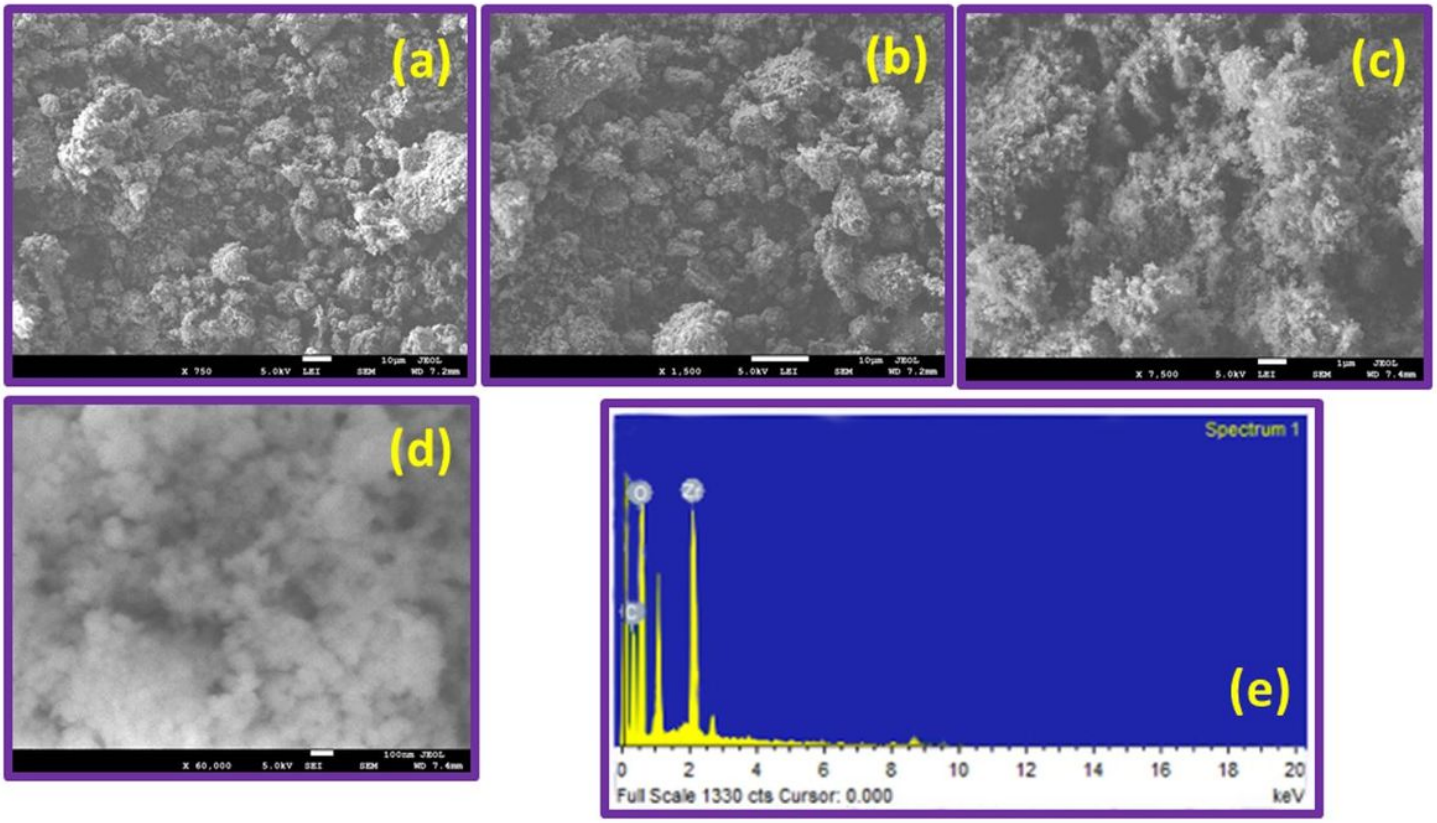

Figure 3

SEM micrographs of (a, b) CAA at magnifications of (x = 750, 1500); (c, d) Zr-CAA at magnifications of (x = 7500, 60000); (e) EDX analysis of Zr-CAA

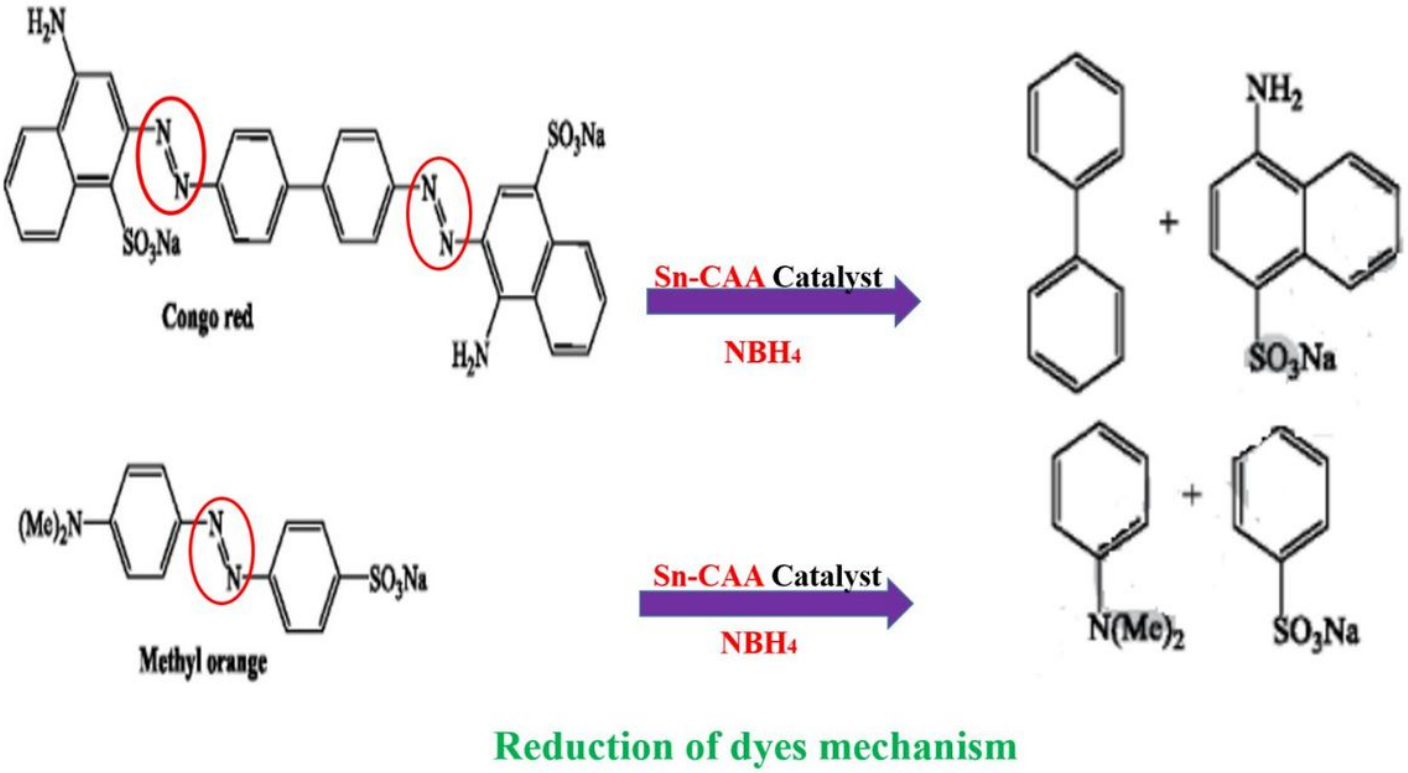

Figure 4

Proposed mechanism of reduction of MO and CR

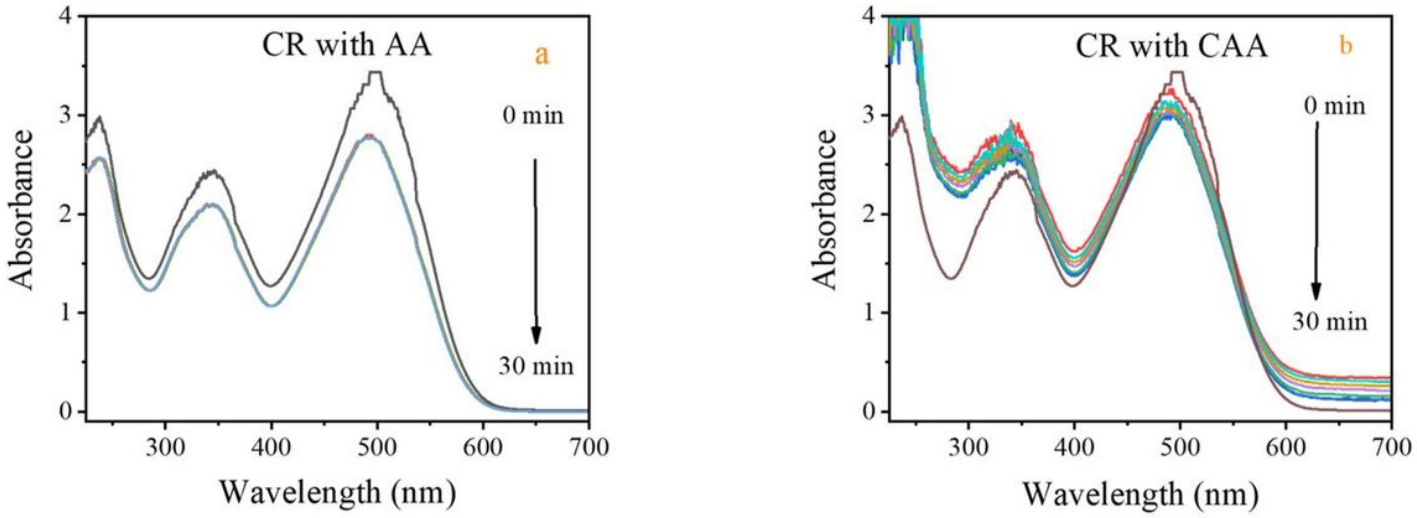

Figure 5

UV-Vis spectra for reduction of C.R by NaBH4 with time in the presence of AA (a) C.R by NaBH4 with time in the presence of CAA (b)

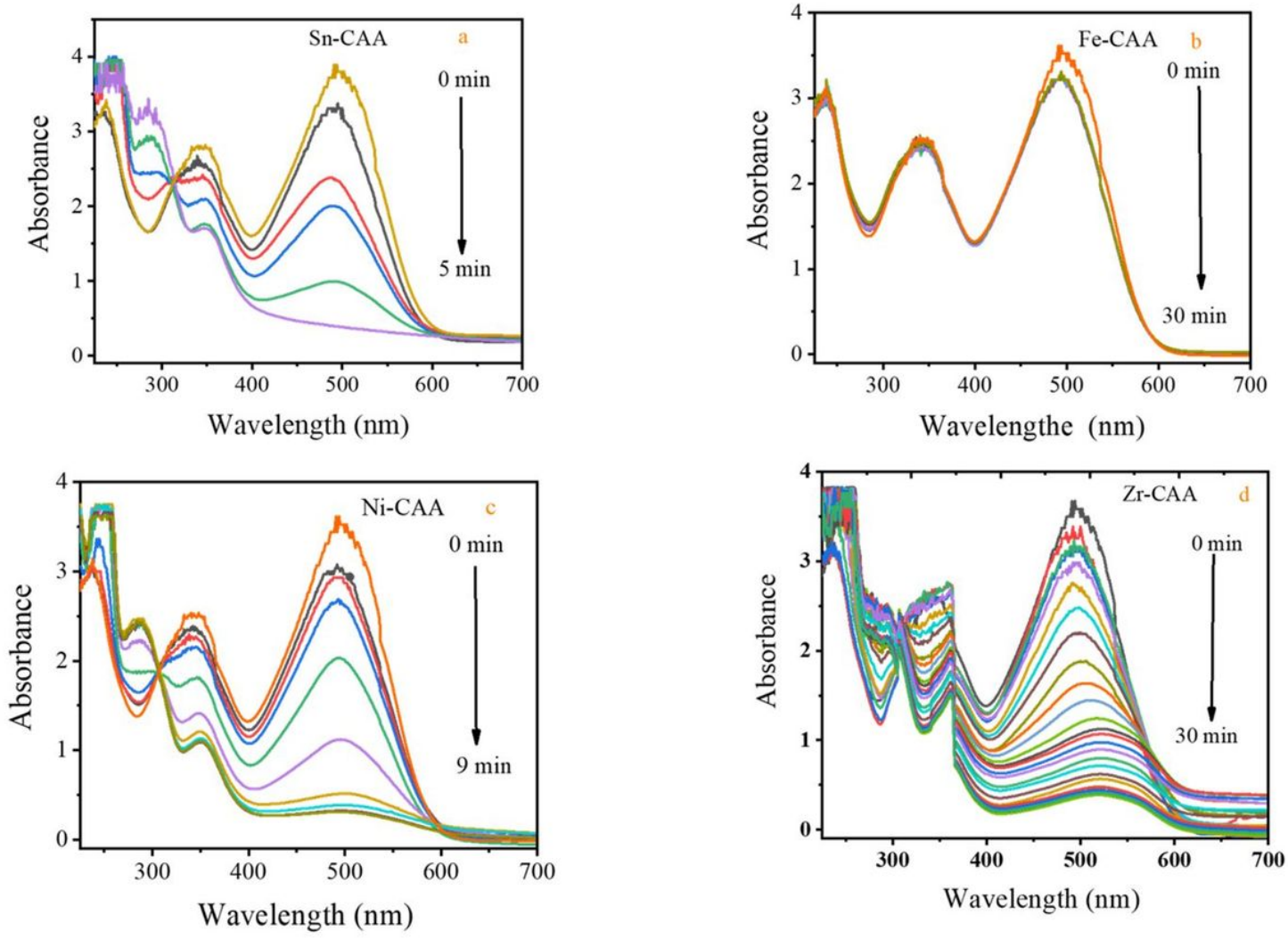

Figure 6

UV-Vis spectra for reduction of CR by NaBH4 with time in the presence of M-CAA catalytic Fe -CAA(a), Sn-CAA (b), Ni-CAA (c), Zr-CAA (d).

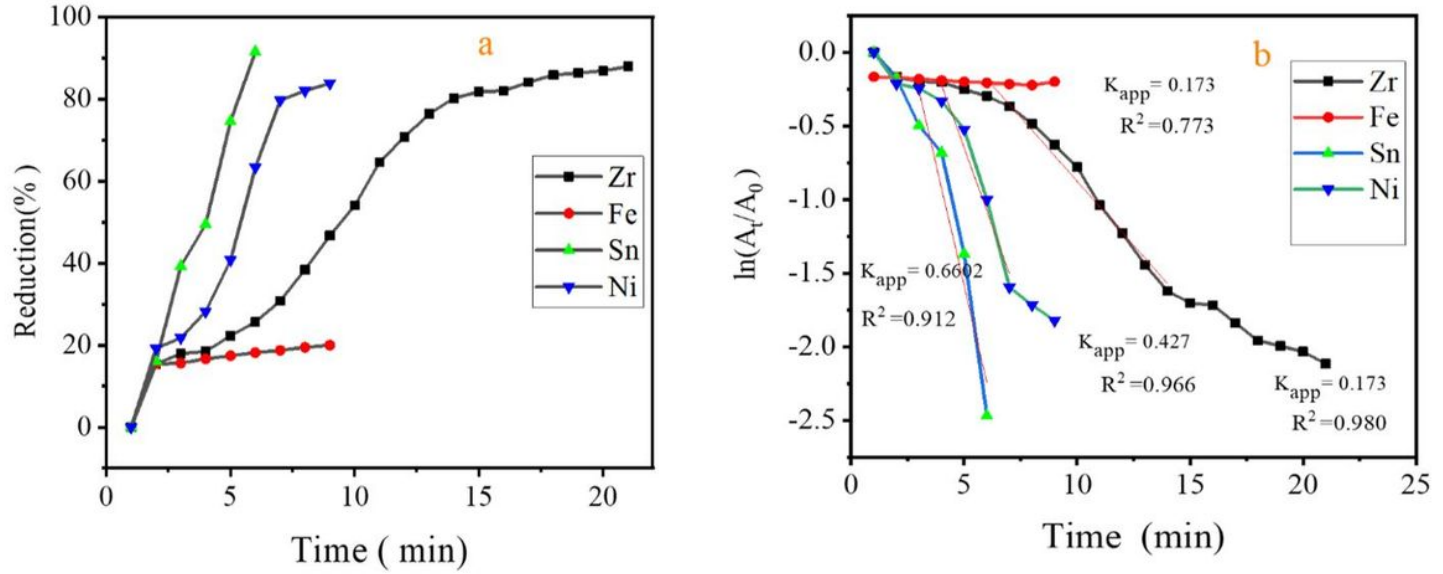

Figure 7

comparative percent reduction of CR, and (d) plot of ln (At/A0) versus time for CR. Experimental conditions (2.5 ml of aqueous dye solution + 0.5 ml of 0.1 M aqueous NaBH4 solution + 10 mg of M-CAA).

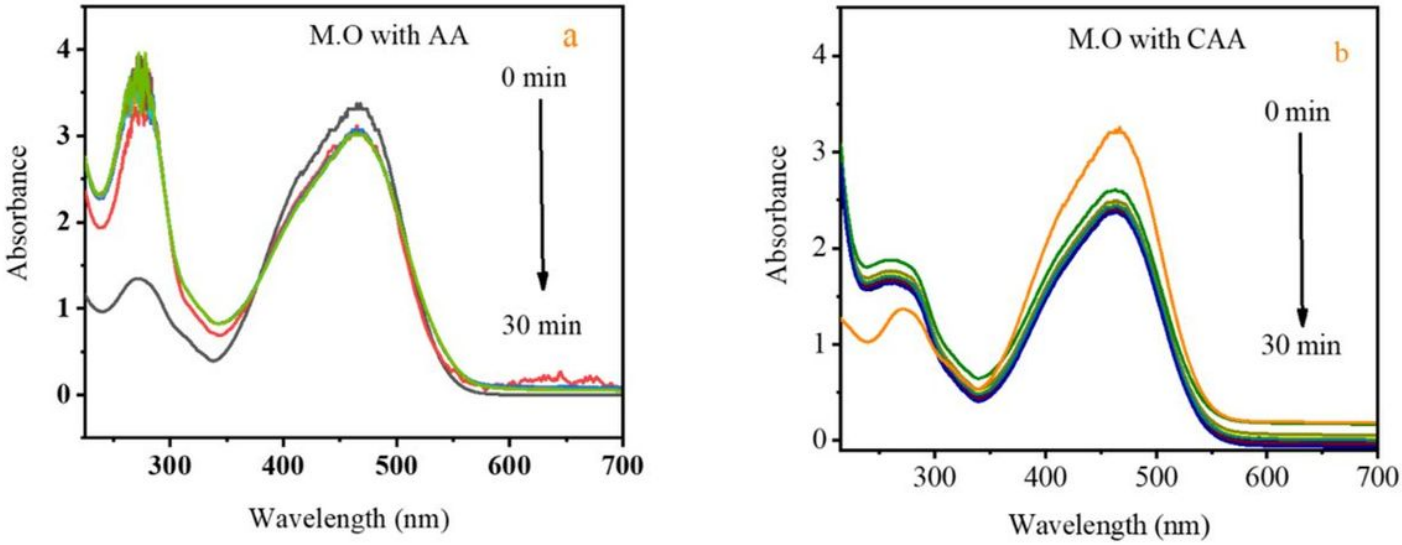

Figure 8

UV-Vis spectra for reduction of MO by NaBH4 with time in the presence of AA (a) MO by NaBH4 with time in the presence of CAA (b)

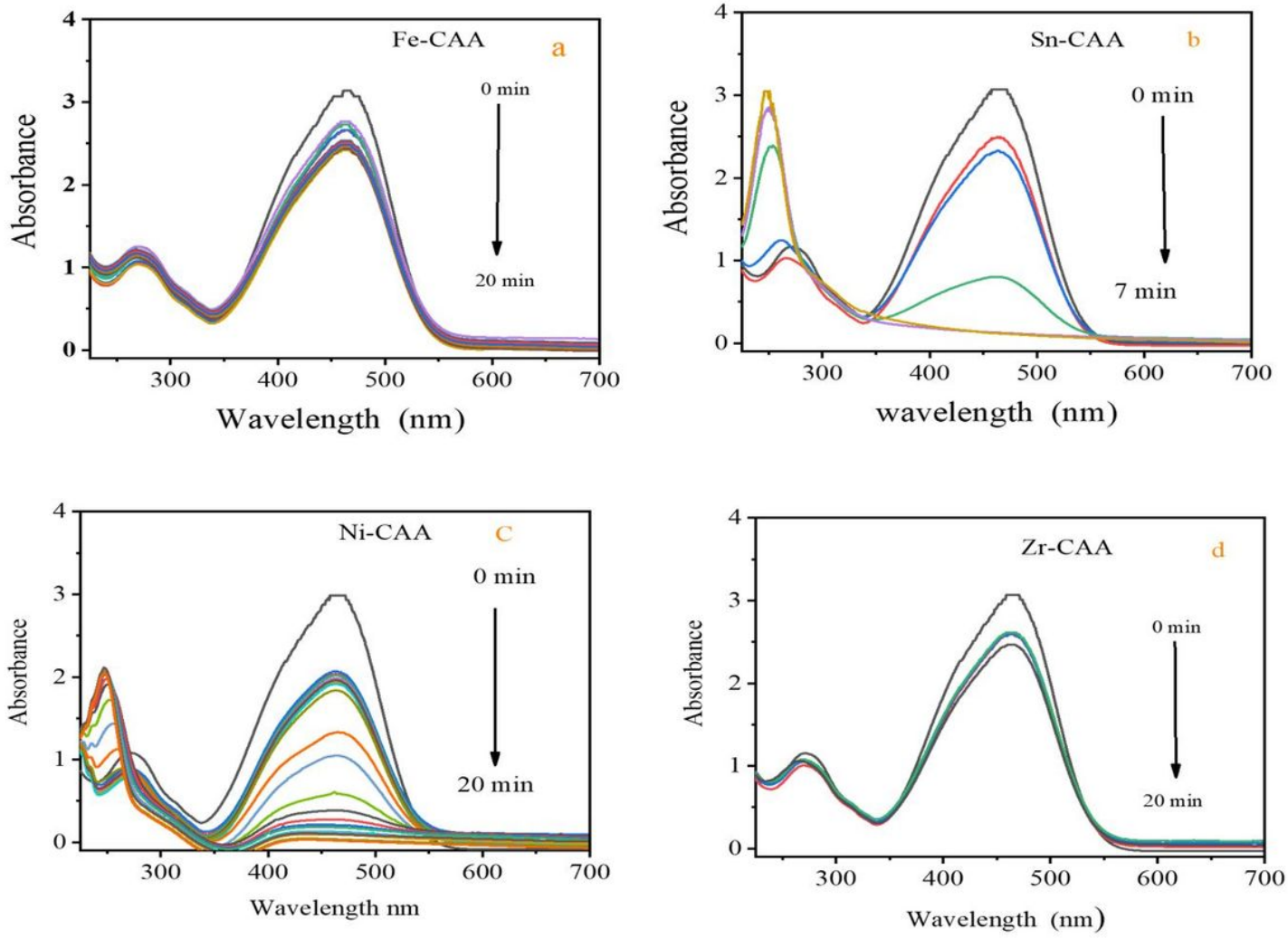

Figure 9

UV-Vis spectra for reduction of M.O by NaBH4 with time in the presence of M-CAA catalytic Sn -CAA(a), Fe -CAA (b), Ni-CAA (c), Zr-CAA (d)

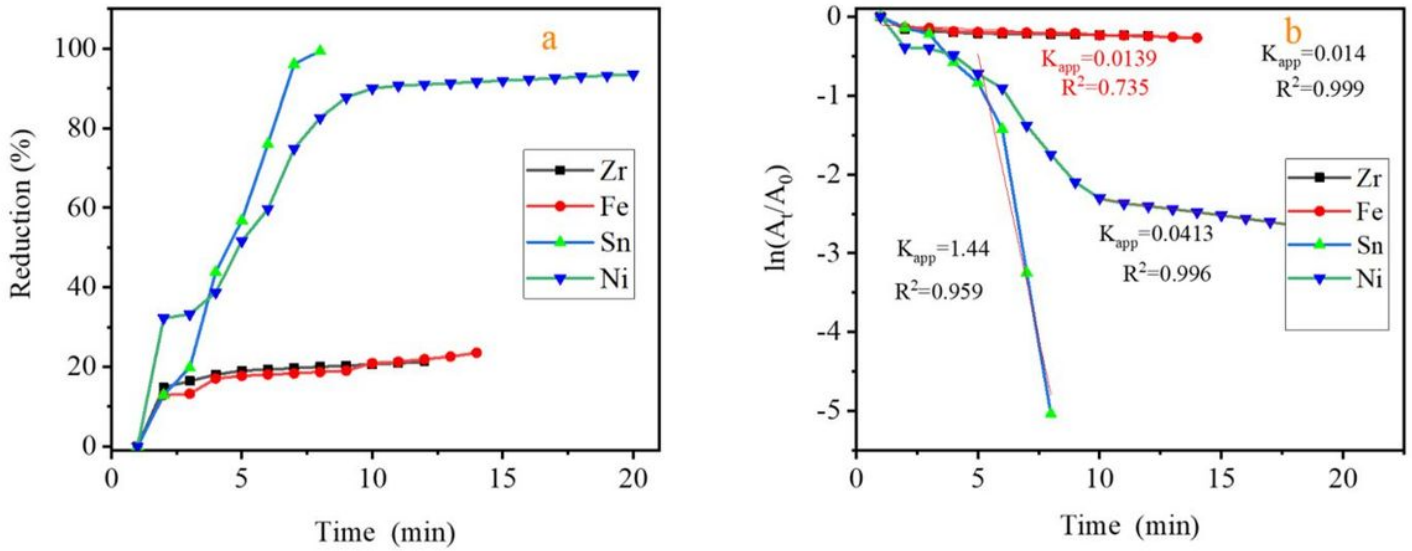

Figure 10

(a)comparative percent reduction of MO, and (b) plot of ln (At/A0) versus time for MO. Experimental conditions (2.5 ml of aqueous dye solution + 0.5 ml of 0.1 M aqueous NaBH4 solution + 10 mg of M-CAA).

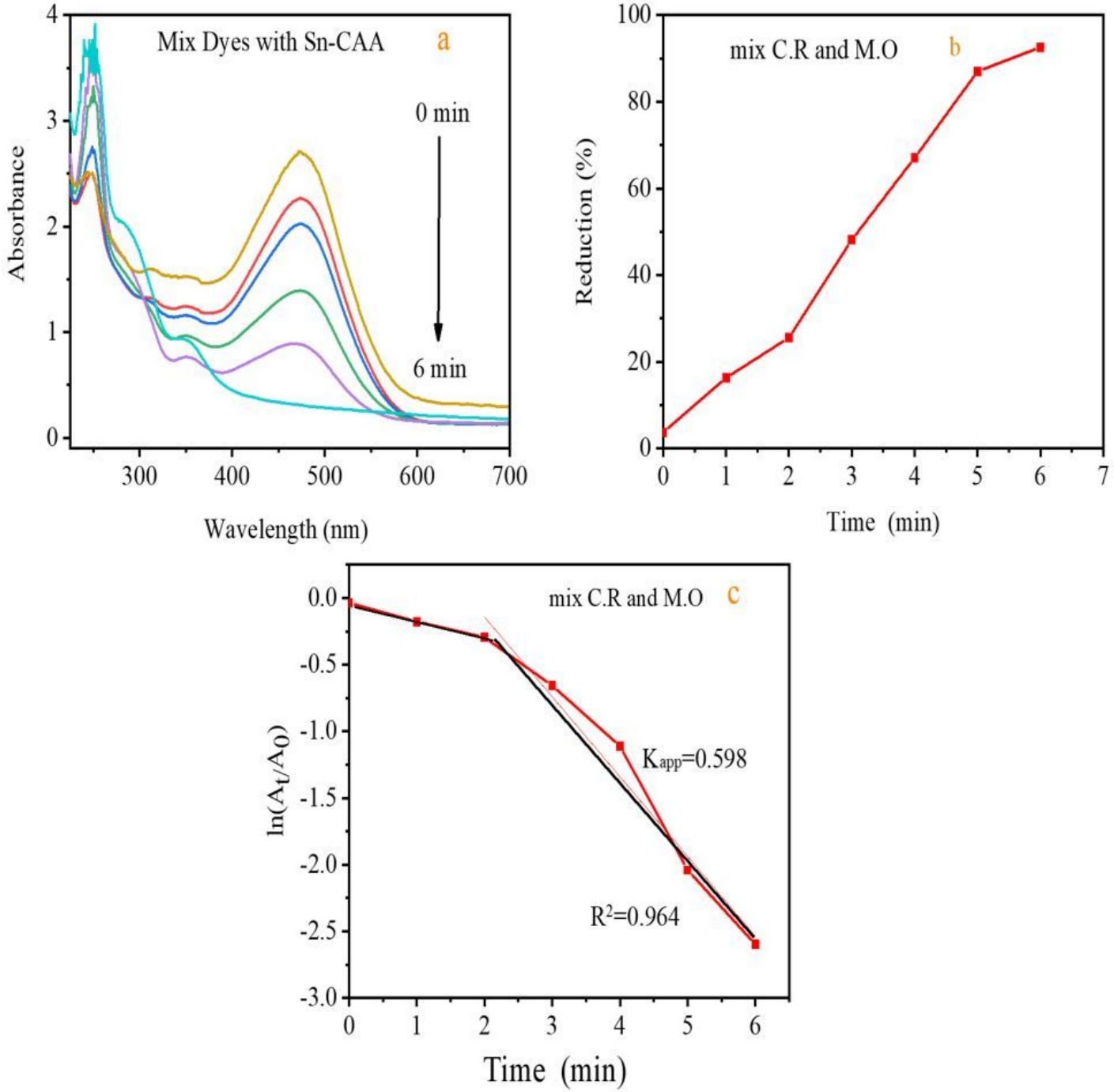

Figure 11

In the presence of Sn-CAA catalyst, UV absorption spectra of mix solution M.O and C.R as a function time(a). percent removal of M.O and C.R in the mixed solution with time (t)(b). ln(At/A0) and K app value

(c)

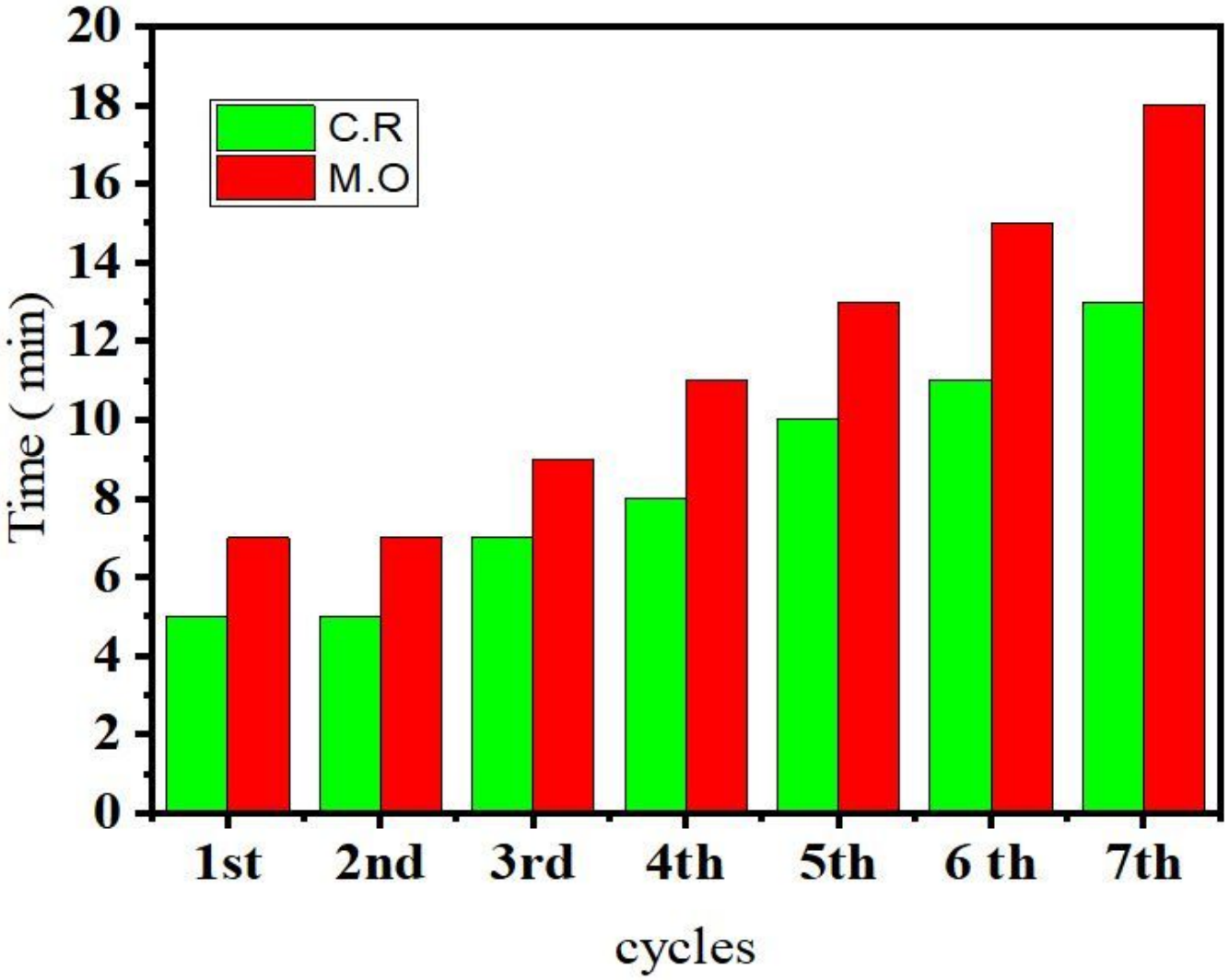

Figure 12

re-use of Sn-CAA catalyst for 7-times reduction of M.O and C.R as a function of time.

Supplementary Files

This is a list of supplementary files associated with this preprint. Click to download.

- graphicsabstract.jpg